not previously been identified as a treatment with an increased risk of PML.

A definitive diagnosis of PML can be based on the concomitant presence of a compatible clinical and neuroimaging picture and characteristic histopathologic features with JCV detection in the brain tissue [11]. However, brain biopsy is an invasive method with considerable risks. In addition, the severity and extent of this disease are so marked that patients with PML are often in a poor clinical condition with an impaired hemostatic system, making noninvasive diagnostic methods highly desirable. Therefore, some studies have developed and validated less-invasive diagnostic methods based on the amplification of the JCV-target DNA from CSF by PCR. Fong et al. [12] showed that the sensitivity and specificity of JCV DNA by PCR were 74 and 96%, respectively, and the positive and negative predictive values were 89.5 and 88.5%, respectively, before the highly active antiretroviral therapy (HAART) era.

The MRI findings in patients with PML present characteristic images. There should be areas of decreased signal intensity on T1-weighted images and increased signal intensity on T2-weighted images [13]. The images are dominated by T2-signal abnormalities of the white matter [3, 14]. This is reflected by a slight tissue swelling in acute lesions and atrophy in end-stage areas during the demyelination process. Most lesions remain hyperintense on T2-weighted images because the tissue water content increases after the replacement of oligodendrocytes by astrocytes. Tissue destruction continues in clinically progressive patients. Generally, the lesions in PML are not contrast-enhanced by gadolinium and do not show a substantial mass effect. DWI reliably distinguishes intracellular edema from interstitial water accumulation. Intracellular edema is seen in acute cell damage, which is usually followed by cell death. Cell death as observed in the periphery of the cerebral lesions is explained as oligodendrocyte necrosis in the areas of demyelination [7].

In a randomized controlled trial involving 57 patients with HIV infection and biopsy-confirmed PML, cytarabine administered either intravenously or intrathecally did not improve the prognosis compared with antiretroviral therapy alone [15]. For PML associated with AIDS, HAART is relatively effective [16]. Although there have been no large-scale clinical trials on treatment for PML in the absence of AIDS, there is evidence that cytarabine decreases JCV replication and multiplication in vitro [17]. There have also been studies on improvement in non-HIV-related PML when cytarabine is given intravenously, intrathecally, or both [18–20]. The most successful of them, an open-label study involving 19 patients who had PML without HIV infection, showed that intravenous cytarabine at a dosage of 2 mg kg^{-1} daily for five consecutive days appeared to stabilize the neurological and functional status in seven patients (36%) at 2–4.5 years of follow-up, despite significant bone marrow toxicity complications [21]. Based on these studies, we chose cytarabine for the treatment of PML in the present case.

A recent study reported that approximately 80% of PML patients have AIDS, 13% have hematological malignancies, 5% are transplant recipients, and 2% have chronic inflammatory diseases [22]. Since 1990, when purine analogs first became available, the incidence of PML has increased [5]. The Food and Drug Administration alert in December 2006 reported that two patients with systemic lupus erythematosus died after treatment with rituximab. Thus, this new class of medication, such as purine analogs and rituximab used in treating hematological malignancies, may increase the number of patients at risk of developing PML [5, 12]. $CD4^+$ T-cell counts of less than 200 μL^{-1} are known to be a risk factor for the development of PML [5]. For those patients with reduced CD4 T-cell counts and T-cell deviations (compromised cellular immunity), the administration of rituximab or the application of the CHOP regimen may impair humoral immunity, which in turn may lead to the onset of PML. For the present patient, the CHOP regimen that preceded rituximab caused a decrease in the IgG level, and the subsequent rituximab administration resulted in a further reduction in IgG (the level ultimately reaching 391 mg/dL). It was suggested that the R-CHOP regimen may compromise humoral immunity in patients with a reduced $CD4^+$ T-cell count and expose them to a risk of developing PML or other opportunistic infections. This was true in our case: our patient's $CD4^+$ T-cell count before R-CHOP therapy was 68 μL^{-1}. Thus, when a variegated neurological symptom is noted during rituximab-containing chemotherapy, one must consider the possibility of PML while making a differential diagnosis.

Acknowledgment This study was supported in part by grants from the Ministry of Health, Labor, and Welfare, Japan.

References

1. Koralnik IJ. New insights into progressive multifocal leukoencephalopathy. Curr Opin Neurol. 2004;17:365–70.
2. Padgett BL, Walker DL, ZuRhein GM, Eckroade RJ, Dessel BH. Cultivation of papova-like virus from human brain with progressive multifocal leucoencephalopathy. Lancet. 1971;1:1257–60.
3. Berger JR, Major EO. Progressive multifocal leukoencephalopathy. Semin Neurol. 1999;19:193–200.
4. Vidarsson B, Mosher DF, Salamat MS, Isaksson HJ, Onundarson PT. Progressive multifocal leukoencephalopathy after fludarabine therapy for low-grade lymphoproliferative disease. Am J Hematol. 2002;70:51–4.
5. García-Suárez J, de Miquel D, Krsnik I, Banas H, Arribas I, Burqaleta C. Changes in the natural history of progressive

multifocal leukoencephalopathy in HIV-negative lymphoproliferative disorders: Impact of novel therapies. Am J Hematol. 2005;80:271–81.
6. Gasnault J, Kahraman M, de Herve MG, Durali D, Delfraissy JF, Taoufik Y. Critical role of JC virus-specific CD4 T-cell responses in preventing progressive multifocal leukoencephalopathy. AIDS. 2003;17:1443–9.
7. Major EO, Amemiya K, Tormatore CS, Houff SA, Berger JR. Pathogenesis and molecular biology of progressive multifocal leukoencephalopathy, the JC virus-induced demyelinating disease of the human brain. Clin Microbiol Rev. 1992;5:49–73.
8. Fong IW, E Toma. The natural history of progressive multifocal leukoencephalopathy in patients with AIDS Canadian PML Study Group. Clin Infect Dis. 1995;2:1305–10.
9. Smith DK, Neal JJ, Holmberg SD. Unexplained opportunistic infections and $CD4^+$ T lymphocytopenia without HIV infection: an investigation of cases in the United States. The Centers for Disease Control Idiopathic $CD4^+$ T lymphocytopenia Task Force. N Engl J Med. 1993;328:373–9.
10. Goldberg SL, Pecora AL, Alter RS, et al. Unusual viral infections (progressive multifocal leukoencephalopathy and cytomegalovirus disease) after high-dose chemotherapy with autologous blood stem cell rescue and peritransplantation rituximab. Blood. 2002;99:1486–8.
11. Gibson PE, Gardner SD, Field AM. Use of a molecular probe for detecting JCV DNA directly in human brain material. J Med Virol. 1986;18:87–95.
12. Fong IW, Britton CB, Luinstra KE, Toma E, Mahony JB. Diagnostic value of detecting JC virus DNA in cerebrospinal fluid of patients with progressive multifocal leukoencephalopathy. J Clin Microbiol. 1995;33:484–6.
13. Whiteman ML, Post MJ, Berger LG, Tate LG, Bell MD, Limonte LP. Progressive multifocal leukoencephalopathy in 47 HIV-seropositive patients: Neuroimaging with clinical and pathologic correlation. Radiology. 1993;187:233–40.
14. Post MJ, Yiannoutsos C, Simpson D, et al. Progressive multifocal leukoencephalopathy in AIDS: are there any MR findings useful to patient management and predictive of patient survival? AIDS Clinical Trials Group, 243 Team. AJNR Am J Neuroradiol. 1999;20:1896–906.
15. Hall CD, Dafni U, Simpson D, et al. Failure of cytarabine in progressive multifocal leukoencephalopathy associated with human immunodeficiency virus infection. AIDS Clinical Trials Group 243 Team. N Engl J Med. 1998;338:1345–51.
16. Dworkin MS. A review of progressive multifocal leukoencephalopathy in persons with and without AIDS. Curr Clin Top Infect Dis. 2002;22:181–95.
17. Hou J, Major EO. The efficacy of nucleoside analogs against JC virus multiplication in a persistently infected human fetal brain cell line. J Neurovirol. 1998;4:451–6.
18. Bauer WR, Turel AP Jr, Johnson KP. Progressive multifocal leukoencephalopathy and cytarabine: remission with treatment. JAMA. 1973;226:174–6.
19. Marriott PJ, O'Brien MD, Mackenzie IC, Janota I. Progressive multifocal leucoencephalopathy: remission with cytarabine. J Neurol Neurosurg Psychiatry. 1975;38:205–9.
20. O'Riordan T, Daly PA, Hutchinson M, Shattock AG, Gardner SD. Progressive multifocal leukoencephalopathy—remission with cytarabine. J Infect. 1990;20:51–4.
21. Aksamit AJ. Treatment of non-AIDS progressive multifocal leukoencephalopathy with cytosine arabinoside. J Neurovirol. 2001;7:386–90.
22. Koralnik IJ, Schellingerhout D, Frosch MP. Case records of the Massachusetts General Hospital. Weekly clinicopathological exercises. Case 14–2004. A 66-year-old man with progressive neurologic deficits. N Engl J Med. 2004;350:1882–93.

Phase I and II pharmacokinetic and pharmacodynamic study of the proteasome inhibitor bortezomib in Japanese patients with relapsed or refractory multiple myeloma

Yoshiaki Ogawa,[1,4] Kensei Tobinai,[2] Michinori Ogura,[3] Kiyoshi Ando,[1] Takahide Tsuchiya,[1] Yukio Kobayashi,[2] Takashi Watanabe,[2] Dai Maruyama,[2] Yasuo Morishima,[3] Yoshitoyo Kagami,[3] Hirofumi Taji,[3] Hironobu Minami,[4] Kuniaki Itoh,[4] Masanobu Nakata[4] and Tomomitsu Hotta[1]

[1]Department of Hematology and Oncology, Tokai University School of Medicine, 143, Shimokasuya, Isehara, Kanagawa, 259-1193; [2]Hematology and Stem Cell Transplantation Division, National Cancer Center Hospital, 5-1-1, Tsukiji, Chuo-ku, Tokyo, 104-0045; [3]Department of Hematology and Cell Therapy, Aichi Cancer Center, 1-1, Kanokoden, Chikusa-ku, Nagoya, Aichi, 464-8681; [4]Division of Oncology and Hematology, National Cancer Center Hospital East, 6-5-1, Kashiwanoha, Kashiwa, Chiba, 277-8577, Japan

(Received July 22, 2007/Revised September 6, 2007/Accepted September 9, 2007/Online publication October 29, 2007)

The purpose of this phase I and II study was to evaluate the safety, pharmacokinetics, pharmacodynamics, and efficacy of bortezomib in Japanese patients with relapsed or refractory multiple myeloma. This was a dose-escalation study designed to determine the recommended dose for Japanese patients (phase I) and to investigate the antitumor activity and safety (phase II) of bortezomib administered on days 1, 4, 8, and 11 every 21 days. Thirty-four patients were enrolled. A dose-limiting toxicity was febrile neutropenia, which occurred in one of six patients in the highest-dose cohort in phase I and led to the selection of 1.3 mg/m^2 as the recommended dose. Adverse events ≥ grade 3 were rare except for hematological toxicities, although there was one fatal case of interstitial lung disease. The overall response rate was 30% (95% confidence interval, 16–49%). Pharmacokinetic evaluation showed a biexponential decline, characterized by a rapid distribution followed by a longer elimination, after dose administration, whereas the area under the concentration–time curve increased proportionately with the dose. Bortezomib was effective in Japanese patients with relapsed or refractory multiple myeloma. A favorable tolerability profile was also seen, although the potential for pulmonary toxicity should be monitored closely. The pharmacokinetic and pharmacodynamic profiles of bortezomib in the present study warrant further investigations, including more relevant administration schedules. (*Cancer Sci* 2008; 99: 140–144)

Multiple myeloma, one of the B-cell lymphatic tumors, is a malignant hematopoietic tumor with poor prognosis for which a cure cannot ever be expected. The peak age of onset is high at 65–70 years, and its onset in patients younger than 40 years is rare. The median survival of patients with multiple myeloma is approximately 6–12 months if untreated, but it is prolonged to approximately 3 years with the administration of chemotherapy; the 5-year survival rate has been reported to be approximately 25% and the 10-year survival rate is <5%.[1,2] As initial therapy for multiple myeloma, melphalan + prednisolone therapy and vincristine + doxorubicin + dexamethasone therapy have been used as global standards.[3,4] High-dose chemotherapy combined with autologous hematopoietic stem-cell transplantation is reported to be significantly superior to multiagent chemotherapy in terms of response rate and progression-free survival,[5] and is considered to be a standard therapy primarily for patients who are 65 years old or younger. However, no consensus has been reached on the standard therapy for relapsed or chemotherapy-refractory multiple myeloma patients.[6–8] Multiple myeloma is an intractable disease with poor prognosis that continues to relapse, and the duration to relapse becomes shorter in patients who repeatedly receive treatment. There are no available treatment options in which durable efficacy can be expected after relapse, and therefore effective therapeutic choices with new mechanisms of action have been long awaited.

Bortezomib is a novel small molecule that is a potent selective and reversible inhibitor of the proteasome, and has been approved for the treatment of recurrent or refractory multiple myeloma in the USA and Europe. The pharmacokinetics (PK) of bortezomib were reported in a phase I study in which it was administered in combination with gemcitabine twice weekly for 2 weeks followed by a 10-day rest period,[9] and in another phase I study in which it was administered once weekly for 4 weeks followed by a 13-day rest period.[10] Both studies were conducted in patients with advanced solid tumors and not patients with multiple myeloma. Therefore, the present phase I and II study was designed to assess the PK and pharmacodynamic (PD) effects of bortezomib in multiple myeloma patients, particularly in a Japanese population. In addition, efficacy and safety were evaluated to determine the recommended dose (RD).

Patients and Methods

Eligibility. The main eligibility criteria were: confirmed multiple myeloma according to the South-west Oncology Group diagnostic criteria;[11] had received at least previous standard front-line therapy (including melphalan and predonisone, vincristine, doxorubicin, and dexamethasone chemotherapy, and high-dose chemotherapy with autologous stem cell transplantation); had documentation of relapse or refractoriness to the last line of therapy and required therapy because of progressive disease at enrolment. Progressive disease was defined as at least one of the following: more than 25% increase in monoclonal immunoglobulin in the serum or urine; development of new osteolytic lesions or soft tissue tumors, or worsening of existing lesions; hypercalcemia (corrected serum calcium value of >11.5 mg/dL); relapse from complete response (CR); the presence of measurable disease lesions; Karnofsky performance status ≥ 60; 20–74 years of age; adequate bone marrow function (absolute neutrophil count ≥ 1000/mm^3, platelets ≥ 75 000/mm^3, and hemoglobin ≥ 8 g/dL),

*To whom correspondence should be addressed.
E-mail: yoshioga@is.icc.u-tokai.ac.jp

doi: 10.1111/j.1349-7006.2007.00638.x

hepatic function (aspartate aminotransferase and alanine aminotransferase levels ≤2.5 times the upper limit of institutional normal range, total bilirubin ≤1.5 times the upper limit of institutional normal range), renal function (creatinine clearance ≥ 30 mL/min), and cardiac function (left ventricular ejection fraction ≥ 55% by echocardiography without New York Heart Association class III to IV congestive heart failure) in the previous 2 weeks; and had received no systemic chemotherapy or radiotherapy in the previous 4 weeks. This study was approved by the Institutional Review Board of each participating hospital. All patients gave written informed consent and the study was conducted in accordance with Good Clinical Practice for Trials of Drugs and the Declaration of Helsinki.

Study design. The RD was determined based on the occurrence of dose-limiting toxicity (DLT) in Japanese patients and in the dose-escalating phase I of the study. The safety and efficacy of bortezomib at the RD were assessed in phase II. In phase I, three patients were enrolled in the 0.7 mg/m^2-dose group, and six patients each in the 1.0 and 1.3 mg/m^2-dose groups. DLT was defined as ≥grade 3 non-hematological toxicity or grade 4 hematological toxicity for which the relation to bortezomib could not be ruled out. The RD was defined as a dose level with a DLT incidence closest to but lower than the estimated (expected) value of 30%. Bortezomib was administered for up to six cycles.

Drug administration. Bortezomib, supplied by Janssen Pharmaceutical (Tokyo, Japan) in vials containing 3.5 mg, was administered by intravenous push over 3–5 s on days 1, 4, 8, and 11, followed by a 10-day rest period, with this 3-week period comprising one cycle. There was an interval of at least 72 h between doses.

Response and safety assessments. Patients were monitored for response after every two treatment cycles by quantitation of serum immunoglobulins, serum protein electrophoresis and immunofixation (IF), and collection of a 24-h urine specimen for total protein, electrophoresis, and IF. Response was evaluated using the European Group for Blood and Marrow Transplantation criteria,[12] after cycles 2, 4, and 6.

Adverse events were assessed and graded according to the National Cancer Institute Common Toxicity Criteria version 2.0 from the first dose until 28 days after the last dose of bortezomib.

Pharmacokinetic and pharmacodynamic analysis. Plasma bortezomib concentrations and blood 20S proteasome activity were measured in phase I. Blood samples were collected before each dose, at 5, 15, and 30 min, and 1, 2, 4, 6, 8, 12, 24, and 48 h after treatment on days 1 and 11. The measurement of plasma bortezomib concentration was conducted at Advion BioSciences (Ithaca, NY, USA) using liquid chromatography/tandem mass spectrometry (LC/MS/MS).[13] The measurement of blood 20S proteasome activity was conducted at Millennium Pharmaceuticals (Cambridge, MA, USA) using the synthetic fluorescence substrate method validated for the chymotrypsin-like activity/trypsin-like activity ratio.[14]

Results

Patients and dose escalation. The study was conducted from May 2004 to January 2006, and 34 patients were enrolled. Patient characteristics are shown in Table 1. All patients had secretory-type myeloma, and the breakdown was 20 patients (59%) with IgG type, eight patients (24%) with IgA type, three patients (9%) with light-chain type, and three patients (9%) with IgA and light-chain type. Most patients had received prior therapy with steroids, alkylating agents, and/or vinca alkaloids. Ten patients (29%) had received stem cell transplantation including high-dose therapy. The median number of lines of prior therapy was two (range: one to eight). Osteolytic lesions were observed in 30 patients (88%) and soft-tissue tumors were observed in seven (21%). The median number of treatment cycles was four (range: one to six), and the median duration of treatment was 79 days (range: 1–152 days). Ten patients (29%) completed all six cycles. The reasons for discontinuation of therapy in 25 patients were progressive disease in 11 patients, patient's own request in six patients, serious adverse events in four patients, DLT in two patients, and others in three patients. Three patients were enrolled in the 0.7 mg/m^2 group and six in the 1.0 mg/m^2 group, and no DLT were observed at any dose level. In the 1.3 mg/m^2 group, DLT (grade 3 febrile neutropenia) occurred in one of the six patients. Therefore, 1.3 mg/m^2 was determined to be the RD in subsequent phase II, in which 18 patients were enrolled.

Table 1. Patient characteristics

Patient characteristic	n	%
Patients	34	
Sex		
Female	12	35
Male	22	65
Age (years)		
Median	60	
Range	34–72	
Durie-Salmon stage		
I	0	
II	15	44
III	19	56
Time since diagnosis (years)		
Median	3.4	
Range	1.0–13.7	
Karnofsky performance status		
100	15	44
90–80	18	53
70–60	1	3
Serum interleukin-6 (pg/mL)		
Mean	4.2	
Range	0.5–30.2	
Cytogenetics		
Karyotype abnormal	4	12
del(13)(q14)	7	21
t(11; 14)	4	12
Prior therapy		
Chemotherapy	34	100
Steroids	34	100
Alkylating agents	33	97
Vinca alkaloids	27	79
Anthracyclines	22	65
Thalidomide	8	24
Interferon	7	21
Radiation therapy	6	18
Autologous hematopoietic stem cell transplantation	10	29

Adverse events. The safety analysis dataset consisted of all patients who received at least one dose of bortezomib (34 patients). Adverse events observed in ≥20% of patients are shown in Table 2. The events observed at a high frequency (≥50%) were lymphopenia, neutropenia, leukopenia, thrombocytopenia, anemia, asthenia, diarrhea, constipation, nausea, anorexia, and pyrexia. At least one ≥grade 3 adverse event was observed in 88% of the patients. Major ≥grade 3 adverse events were hematological toxicities including lymphopenia, neutropenia, leukopenia, thrombocytopenia, and anemia. Grade 4 hematological toxicities included neutropenia in six patients (18%), three of which experienced this adverse event during cycle 1. At least grade 3 non-hematological toxicities occurred in fewer than 10%, and no DLT during cycle 1 were observed. Grade 4 non-hematological toxicities included hematuria, blood amylase

Table 2. All adverse events occurring in at least 20% of patients ($n = 34$)

Dose (mg/m²)	0.7		1.0		1.3		All			
No. of Patients	($n = 3$)		($n = 6$)		($n = 25$)		($n = 34$)		Total	%
NCI-CTC grade	1/2	3/4	1/2	3/4	1/2	3/4	1/2	3/4		
Adverse event										
Hematologic										
Lymphopenia	3	0	4	2	8	17	15	19	34	100
Neutropenia	1	1	2	4	7	16	10	21	31	91
Leukopenia	2	0	6	0	11	12	19	12	31	91
Thrombocytopenia	1	0	4	0	12	11	17	11	28	82
Anemia	2	0	2	3	10	8	14	11	25	74
Nonhematological										
Asthenia[1]	3	0	3	0	15	0	21	0	21	62
Diarrhea	1	0	2	0	15	1	18	1	19	56
Constipation	2	0	3	0	14	0	19	0	19	56
Nausea	2	0	2	0	14	0	18	0	18	53
Anorexia	3	0	2	0	14	0	18	0	18	53
Pyrexia	0	0	4	0	14	0	18	0	18	53
Peripheral neuropathy[2]	0	0	3	0	12	1	15	1	16	47
AST increased	1	0	1	0	11	2	13	2	15	44
LDH increased	1	0	1	0	12	1	14	1	15	44
Vomiting	1	0	0	0	9	1	10	1	11	32
Rash	0	0	1	0	10	0	11	0	11	32
ALP increased	0	0	2	0	8	0	10	0	10	29
Headache	0	0	1	0	8	0	9	0	9	27
ALT increased	1	0	1	0	7	0	9	0	9	27
Hyperglycaemia	0	0	2	0	5	0	7	0	7	21
Hyponatremia	1	0	0	1	5	0	6	1	7	21
Renal impairment	1	0	1	0	5	0	7	0	7	21
CRP increased	0	0	1	0	6	0	7	0	7	21
Weight decreased	0	0	0	0	7	0	7	0	7	21

[1]Including fatigue and malaise. [2]Including peripheral sensory neuropathy, peripheral motor neuropathy, and hypoesthesia. ALP, alkaline phosphatase; ALT, alanine aminotransferase; AST, aspartate aminotransferase; CRP, C-reactive protein; LDH, lactate dehydrogenase; NCI-CTC, National Cancer Institute Common Toxicity Criteria.

increase, and blood uric acid increase in one patient (3%) each. Hematuria was attributed to prostate cancer and judged as not related to bortezomib. The underlying disease was considered to be involved in the blood uric acid increase; this event was judged unlikely to be related to bortezomib. At the occurrence of grade 4 blood amylase increase, blood amylase isozymes were pancreatic-type in 86% and salivary-type in 14%. There were no gastrointestinal symptoms, such as abdominal pain, associated with amylase increase. Abdominal echography revealed no finding suggesting pancreatitis or pancreatolithiasis, and the relevant events recovered 5 days after the onset. The causality of the grade 4 blood amylase increase with bortezomib was evaluated as 'probable', and therefore treatment was continued at a reduced dose from 1.3 to 1.0 mg/m².

One case of interstitial lung disease (ILD) that resulted in a fatal outcome was observed in phase II. The patient with grade 5 ILD had developed the event on day 10 in cycle 2 after receiving seven doses of bortezomib in total. Pyrexia, non-productive cough, hypoxia, and dyspnea were observed as early symptoms, and antibiotics, antimicrobials, steroid pulse therapy, and oxygen inhalation were initiated to treat it. However, respiratory failure worsened, so the patient was put on a ventilator, and the study was discontinued. After the onset of ILD, bronchoalveolar lavage was conducted, but the causative pathogen could not be identified. The available examinations for β-D-glucan, cytomegalovirus antigenemia, influenza virus, and urinary antigen of *Legionella* were found to be negative. The diagnosis from the pathological findings was diffuse alveolar damage. A retrospective analysis of the pretreatment computed tomography (CT) images indicated that the patient had subtle interstitial shadows in the basal region of both lungs. In response, the protocol was amended to exclude patients with abnormal pretreatment bilateral interstitial shadows on CT. No cases of fatal pulmonary toxicity were observed thereafter.

Efficacy. Thirty-three patients were evaluable for efficacy, excluding one ineligible patient who had another malignancy (prostate cancer). Objective responses were observed in 10 of 33 patients (30%; 95% confidence interval 16–49%), including five IF-positive complete responses (CR^{IF+}) and five partial responses. Of the 10 responders, five patients had one line of prior therapy, two patients had three lines of prior therapy, and three patients had four or more lines of prior therapy. It is noteworthy that one patient who had received eight lines of prior therapy, including high-dose chemotherapy with autologous stem-cell transplantation, showed CR^{IF+}. Of the 10 patients who had received prior autologous hematopoietic stem cell transplantation, two patients showed CR^{IF+}, and three patients showed PR. With respect to osteolytic lesions, which is one of the efficacy endpoints, partial regression in five patients, partial disappearance in one patient, and regression of soft-tissue tumors in two patients were observed.

Pharmacokinetics and pharmacodynamics. The mean plasma bortezomib concentration–time profiles on days 1 and 11 obtained from 16 patients enrolled in phase I are shown in Fig. 1a. PK parameters obtained using non-compartmental analysis are shown in Table 3. The plasma bortezomib concentration–time

doi: 10.1111/j.1349-7006.2007.00638.x

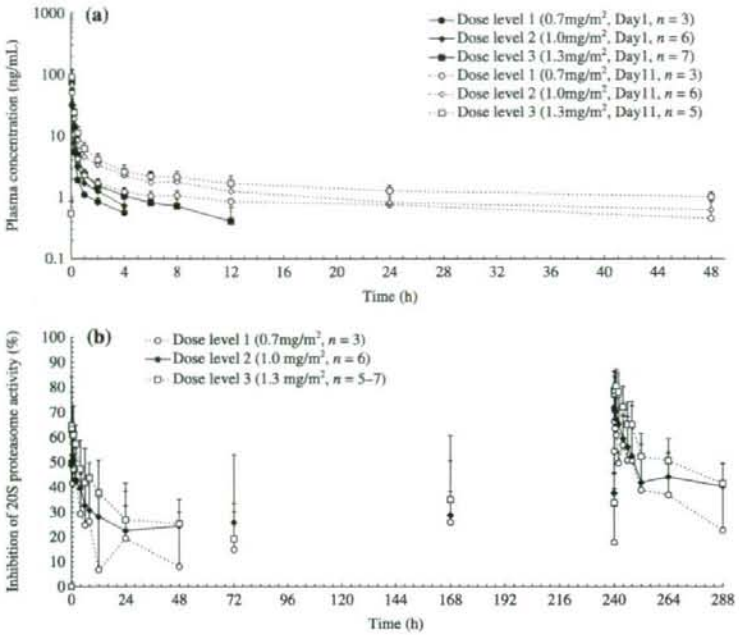

Fig. 1. (a) Plasma bortezomib concentrations (mean + SD). (b) Inhibition of blood 20S proteasome activity (mean + SD).

Table 3. Pharmacokinetic parameters (non-compartmental analysis)

Parameter	Day	Dose (mg/m²) 0.7 (n = 3)	1.0 (n = 6)	1.3 (n = 5–7)†
C_0 (ng/mL)	1	73.75 ± 7.89	144.92 ± 179.31	185.84 ± 57.65
	11	130.68 ± 71.97	147.19 ± 72.33	187.03 ± 54.31
AUC	1	14.04 ± 0.70	28.58 ± 24.86	46.50 ± 19.89
(ng · h/mL)	11	112.01 ± 47.74	108.39 ± 52.32	186.60 ± 49.79
Half life (h)	1	3.31 ± 0.88	6.81 ± 8.81	16.11 ± 20.75
	11	64.59 ± 30.29	32.46 ± 12.91	57.39 ± 24.92
Clearance	1	83.35 ± 10.52	105.41 ± 75.66	51.97 ± 18.99
(L/h)	11	11.77 ± 4.67	19.63 ± 14.50	12.10 ± 3.73
V_z (L)	1	406.92 ± 154.03	520.08 ± 349.87	894.41 ± 682.35
	11	978.51 ± 263.13	731.69 ± 242.35	957.81 ± 350.40
V_{ss} (L)	1	186.46 ± 85.02	288.90 ± 260.74	507.75 ± 558.30
	11	812.60 ± 202.03	540.03 ± 218.72	763.81 ± 271.64
C_0 ratio	11/1	1.789 ± 0.973	1.848 ± 1.133	1.103 ± 0.249
AUC ratio	11/1	7.940 ± 3.247	5.363 ± 2.970	5.142 ± 0.543

†Day 1, n = 7; day 11, n = 5. Values are mean ± SD. AUC, area under the concentration–time curve from time zero to infinity; AUC ratio, AUC on day 11/AUC on day 1; C_0, plasma concentration at the end of administration; C_0 ratio, C_0 on day 11/C_0 on day 1; V_z, the apparent volume of distribution during the terminal phase; V_{ss}, the apparent volume of distribution at steady state.

profiles showed a biphasic elimination profile, characterized by rapid distribution followed by a longer elimination at all dose levels. At any dose level, the elimination half-life ($t_{1/2}$) on day 11 was prolonged, and systemic clearance (CL) was lower compared with day 1. Therefore, delayed elimination of bortezomib from plasma associated with repeated administrations was observed, and the plasma bortezomib concentration after administration (C_0, estimated value) and area under the plasma concentration–time curve (AUC) showed higher values on day 11 compared with day 1. AUC showed dose dependency, whereas C_0 did not.

The inhibition of blood 20S proteasome activity is shown in Fig. 1b. The 20S proteasome inhibition recovered over time at all dose levels, but was prolonged compared with the temporal decrease in plasma bortezomib concentration, and the inhibition was still observed before treatment on days 4, 8, and 11.

Discussion

In the present study, bortezomib was generally well tolerated in the 25 Japanese patients whose treatments were started at the RD of 1.3 mg/m². Hematological toxicities, gastrointestinal toxicities, and peripheral neuropathies observed in our patients were similar to those reported for patients in clinical studies from the USA and Europe.[15,16] Most could be managed without interventions or with the usual symptomatic therapy. Grade 4 neutropenia was observed in 18% of patients, but treatment could be continued with dose reduction. The response rate obtained in the present study was comparable to that reported by Richardson *et al.* in a pivotal phase III study.[16] In addition, patients who had received heavy prior therapy also showed a consistent response. Therefore, 1.3 mg/m² is considered appropriate as an initial dose of bortezomib in Japanese patients. There was a fatal pulmonary disorder event (ILD) in one patient treated with the 1.3 mg/m² dose in which a causal relationship with bortezomib could not be ruled out. Hence, special care should be taken prior to initiating treatment with bortezomib to evaluate patients (e.g. chest X-ray or chest CT scan) and during and after bortezomib treatment if they develop subjective symptoms such as dyspnea, cough, and fever.

The assessment of PK and PD in multiple myeloma patients treated with bortezomib twice weekly for 2 weeks was conducted for the first time in Japanese patients. A decrease in CL associated with increased exposures and subsequently longer $t_{1/2}$ values were observed after repeated administration and dose escalation. The relatively large volume of distribution suggests that bortezomib may be distributed extensively into the extravascular tissues. It can be postulated that CL values on day 1 are apparent values observed due to rapid tissue distribution, whereas

saturation of proteasome binding sites and tissue distribution occur after multiple dosing, and the CL value on day 11 may be a better representation of the true value.

It was also found that the blood 20S proteasome inhibition at each dose level recovered over time, but was prolonged compared with the temporal decrease in plasma bortezomib concentration. Similarly to CL, this could be due to the large distribution volume of bortezomib and its slow return from tissues to plasma.

Delayed elimination and enhanced proteasome inhibition were observed with repeated administration and dose increase, but no clear tendency in the incidence or degree of adverse reactions was observed. However, the PD results of the present study in Japanese patients demonstrate that the inhibition of 20S proteasome activity does not recover even after 72 h, which is specified as a minimum interval for bortezomib dosing. Accordingly, when bortezomib is used in clinical practice, it is important to determine the optimal dosage and determine whether it is appropriate to administer bortezomib while considering the balance between safety and efficacy.

Acknowledgments

We thank all of the investigators, physicians, nurses, and clinical research coordinators at Tokai University School of Medicine, National Cancer Center Hospital, Aichi Cancer Center, and National Cancer Center Hospital East. We give recognition to Dr A. Togawa (Kofu National Hospital, Kofu, Japan), Dr Y. Sasaki (Saitama Medical University, Saitama, Japan), and Dr K. Hatake (Cancer Institute Hospital, Japanese Foundation for Cancer Research, Tokyo, Japan) for their strict review of the clinical data as members of the Independent Data Monitoring Committee.

References

1 Oken MM. Standard treatment of multiple myeloma. *Mayo Clin Proc* 1994; **69**: 781–6.
2 Oken MM. Management of myeloma: current and future approaches. *Cancer Control* 1998; **5**: 218–25.
3 Paccagnella A, Chiarion-Sileni V, Soesan M *et al*. Second and third responses to the same induction regimen in relapsing patients with multiple myeloma. *Cancer* 1991; **68**: 975–80.
4 Attal M, Harousseau J, Stoppa J *et al*. A prospective, randomized trial of autologous bone marrow transplantation and chemotherapy in multiple myeloma. *N Eng J Med* 1996; **335**: 91–7.
5 Child JA, Morgan GJ, Davies FE *et al*. High-dose chemotherapy with hematopoietic stem-cell rescue for multiple myeloma. *N Engl J Med* 2003; **348**: 1875–83.
6 Barlogie B, Smith L, Alexanian R. Effective treatment of advanced multiple myeloma refractory to alkylating agents. *N Engl J Med* 1984; **310**: 1353–6.
7 Alexanian R, Barlogie B, Dixon D. High-dose glucocorticoid treatment of resistant myeloma. *Ann Intern Med* 1986; **105**: 8–11.
8 Buzaid AC, Durie BG. Management of refractory myeloma: a review. *J Clin Oncol* 1988; **6**: 889–905.
9 Appleman LJ, Ryan DP, Clark JW *et al*. Phase 1 dose escalation study of bortezomib and gemcitabine safety and tolerability in patients with advanced solid tumors. *39th Annual Meeting of the American Society of Clinical Oncology* 2003 (abstract 839).
10 Papandreou CN, Daliani DD, Nix D *et al*. Phase I trial of the proteasome inhibitor bortezomib in patients with advanced solid tumors with observations in androgen-independent prostate cancer. *J Clin Oncol* 2004; **22**: 2108–21.
11 Huang Y, Hamilton A, Arnuk OJ, Chaftari P, Chemaly R. Current drug therapy for multiple myeloma. *Drugs* 1999; **57**: 485–506.
12 Blade J, Samson D, Reece D *et al*. Criteria for evaluating disease response and progression in patients with multiple myeloma treated by high-dose therapy and haemopoietic stem cell transplantation. Myeloma Subcommittee of the EBMT. *European Group for Blood Marrow Transplant Br J Haematol* 1998; **102**: 1115–23.
13 Nix DJ, Pien C, LaButti J *et al*. Clinical pharmacology of the proteasome inhibitor PS-341. *AACR-NCI-EORTC International Conference on Molecular Targets and Cancer Therapeutics* 2001 (abstract 389).
14 Lightcap ES, McCormack TA, Pien CS *et al*. Proteasome inhibition measurements: clinical application. *Clin Chem* 2000; **46**: 673–83.
15 Richardson PG, Barlogie B, Berenson J *et al*. A phase 2 study of bortezomib in relapsed, refractory myeloma. *N Engl J Med* 2003; **348**: 2609–17.
16 Richardson PG, Sonneveld P, Schuster MW *et al*. Bortezomib or high-dose dexamethasone for relapsed multiple myeloma. *N Engl J Med* 2005; **352**: 2487–98.

doi: 10.1111/j.1349-7006.2007.00638.x

Oncogene (2008) 27, 2249–2256

www.nature.com/onc

ONCOGENOMICS

Identification of the novel *AML1* fusion partner gene, *LAF4*, a fusion partner of *MLL*, in childhood T-cell acute lymphoblastic leukemia with t(2;21)(q11;q22) by bubble PCR method for cDNA

Y Chinen[1,2], T Taki[1], K Nishida[2], D Shimizu[2], T Okuda[2], N Yoshida[2], C Kobayashi[3], K Koike[3], M Tsuchida[3], Y Hayashi[4] and M Taniwaki[1,2]

[1]Department of Molecular Laboratory Medicine, Kyoto Prefectural University of Medicine Graduate School of Medical Science, Kamigyo-ku, Kyoto, Japan; [2]Department of Molecular Hematology and Oncology, Kyoto Prefectural University of Medicine Graduate School of Medical Science, Kamigyo-ku, Kyoto, Japan; [3]Department of Pediatrics, Ibaraki Children's Hospital, Futabadai, Mito, Japan and [4]Gunma Children's Medical Center, Shimohakoda, Hokkitsu, Shibukawa, Gunma, Japan

The *AML1* gene is frequently rearranged by chromosomal translocations in acute leukemia. We identified that the *LAF4* gene on 2q11.2–12 was fused to the *AML1* gene on 21q22 in a pediatric patient having T-cell acute lymphoblastic leukemia (T-ALL) with t(2;21)(q11;q22) using the bubble PCR method for cDNA. The genomic break points were within intron 7 of *AML1* and of *LAF4*, resulting in the in-frame fusion of exon 7 of *AML1* and exon 8 of *LAF4*. The *LAF4* gene is a member of the *AF4/FMR2* family and was previously identified as a fusion partner of *MLL* in B-precursor ALL with t(2;11)(q11;q23), although *AML1-LAF4* was in T-ALL. *LAF4* is the first gene fused with both *AML1* and *MLL* in acute leukemia. Almost all *AML1* translocations except for *TEL-AML1* are associated with myeloid leukemia; however, *AML1-LAF4* was associated with T-ALL as well as *AML1-FGA7* in t(4;21)(q28;q22). These findings provide new insight into the common mechanism of *AML1* and *MLL* fusion proteins in the pathogenesis of ALL. Furthermore, we successfully applied bubble PCR to clone the novel *AML1-LAF4* fusion transcript. Bubble PCR is a powerful tool for detecting unknown fusion transcripts as well as genomic fusion points.

Oncogene (2008) **27,** 2249–2256; doi:10.1038/sj.onc.1210857; published online 29 October 2007

Keywords: *AML1/RUNX1*; *LAF4*; T-cell acute lymphoblastic leukemia; *MLL*

Correspondence: Dr T Taki, Department of Molecular Laboratory Medicine, Kyoto Prefectural University of Medicine Graduate School of Medical Science, 465 Kajii-cho Kawaramachi-Hirokoji, Kamigyo-ku, Kyoto 602-8566, Japan.
E-mail: taki-t@umin.net
Received 4 May 2007; revised 13 September 2007; accepted 17 September 2007; published online 29 October 2007

Introduction

A large number of leukemias have been found to be associated with specific chromosomal aberrations. Recent studies have demonstrated that several chromosomal rearrangements and molecular abnormalities are strongly associated with distinct clinical subgroups and can predict clinical features and therapeutic responses (Rowley, 1999; Taki and Taniwaki, 2006). Some genes have been associated with recurrent rearrangements and have many fusion partner genes, such as *MLL* at 11q23, *TEL (ETV6)* at 12p13 and *NUP98* at 11p15; *AML1* (*RUNX1*, *CBFA2*) at 21q22 is one of the most frequent targets of these chromosomal rearrangements in both acute lymphoblastic leukemia (ALL) and acute myeloid leukemia (AML) (Miyoshi *et al.*, 1991; Hayashi, 2000; Kurokawa and Hirai, 2003). To date, a number of in-frame fusion partners of *AML1* have been cloned: *YTHDF2* at 1p35 (Nguyen *et al.*, 2006), *ZNF687* at 1q21.2 (Nguyen *et al.*, 2006), *MDS1/EVI1* at 3q26 (Mitani *et al.*, 1994), *FGA7* at 4q28 (Mikhail *et al.*, 2004), *SH3D19* at 4q31.3 (Nguyen *et al.*, 2006), *USP42* at 7p22 (Paulsson *et al.*, 2006), *MTG8* (*ETO*, *CBFA2T1*) at 8q22 (Erickson *et al.*, 1992; Miyoshi *et al.*, 1993), *FOG2* at 8q23 (Chan *et al.*, 2005), *TRPS1* at 8q24 (Asou *et al.*, 2007), *TEL* (*ETV6*) at 12p13 (Golub *et al.*, 1995), *MTG16* at 16q24 (Gamou *et al.*, 1998) and *PRDX4* at Xp22 (Zhang *et al.*, 2004). Most *AML1* translocations, except for *TEL-AML1*, are associated with AML, involving the N-terminus Runt domain and lacking the C-terminus transactivation domain (Kurokawa and Hirai, 2003). AML1 fusion proteins are associated with leukemogenesis by dominantly interfering with normal *AML1*-mediated transcription and acting as a transcriptional repressor (Okuda *et al.*, 1998; Wang *et al.*, 1998). Clinically, patients with AML harboring t(8;21) in both children and adults show a high rate of complete remission, and its prognosis is considered better than that of patients with a normal karyotype or other chromosomal aberrations (Grimwade *et al.*, 1998).

In the present study, we analysed pediatric T-ALL with t(2;21)(q11;q22) and identified the *LAF4* gene,

which is one of the fusion partners of *MLL*, as a novel fusion partner of the *AML1* gene.

Results

Case report

A 6-year-old boy with a high leukocyte count ($64\,700\,\mu l^{-1}$), containing 84% blasts in peripheral blood and with a mediastinal mass, was diagnosed as having T-ALL. A bone marrow smear was hypercellular with 69% blasts and negative for myeloperoxidase. The leukemic cells, after gating of CD45-positive cells, were positive for CD5 (90.7%), CD7 (90.7%), CD58 (69.9%) and cytoplasmic CD3 (92.8%), and negative for HLA-DR, IgG, IgM, Igκ, Igλ, CD8, CD13, CD14, CD19, CD20 and CD33. He was treated on the Tokyo Children's Cancer Study Group (TCCSG) L04-16 extremely high-risk (HEX) protocol, including stem cell transplantation, because the response to initial 7-day prednisolone ($60\,mg\,m^{-2}$) monotherapy was poor. He achieved complete remission after the induction phase. After the early consolidation phase and two courses of the consolidation phase, he received allogeneic bone marrow transplantation from an unrelated HLA-matched donor 4 months after diagnosis. He has been in complete remission for 17 months.

The patient's leukemic cells at diagnosis were analysed after written informed consent was obtained from his parents, and the ethics committee of Kyoto Prefectural University of Medicine approved this study.

Identification of the AML1-LAF4 *fusion transcript*

Cytogenetic analysis of the leukemic cells of the patient using routine G-banding revealed 47, XY, add(1)(p36), +der(2)t(2;21)(q13;q22), t(2;21)(q13;q22), −9, −9, +mar1, +mar2, and spectral karyotyping (SKY) analysis revealed 47, XY, der(1)t(1;17)(p36.1;q23), der(2)t(2;21)(q11.2;q22), +der(2)t(2;21)(q11.2;q22), del(5)(p15.1), del(9)(q22), del(9)(p13), der(21)t(2;21)(q11.2;q22) (Supplementary Figure S1). Since *AML1* is located at 21q22, we inferred that *AML1* was rearranged in this case. Fluorescence *in situ* hybridization analysis using *AML1*-specific BAC (bacterial artificial chromosome) clones showed split signals of *AML1* on two der(2)t(2;21)(q11.2;q22) and der(21)t(2;21)(q11.2;q22) chromosomes (Figure 1a).

To isolate fusion transcripts of *AML1*, we performed the bubble PCR method for cDNA (Figure 2) and obtained various-sized products (Figure 3a). Four different-sized products were sequenced and two products contained *AML1* sequences fused to unknown sequences. Basic local alignment search tool (BLAST) search revealed that the unknown sequences were part of the *LAF4* gene and both products had the same in-frame junctions (Figure 3b). *LAF4* was located on chromosome 2q11.2–12, which was compatible with the result of spectral karyotyping analysis. We next performed reverse transcription-PCR to confirm *AML1-LAF4* fusion transcripts, and obtained three different-sized *AML1-LAF4* fusion products, including only one in-frame product (Figures 3c and d); however, reciprocal *LAF4-AML1* fusion transcripts were not generated (Figure 3c). Type 2 transcript is an out-of-frame fusion and generated premature termination in exon 9 of *LAF4* (Figure 3d). On the other hand, type 3 transcript is an in-frame fusion of exon 7 of *AML1* and exon 8 of *LAF4*, the same as the type 1 transcript; however, the type 3 transcript contained an 85-bp intronic sequence between exons 9 and 10 of *LAF4*, which might be due to splicing error, and appeared as a premature termination codon within the intronic sequences (Figure 3d). *AML1-LAF4* fusions were also confirmed by fluorescence *in situ* hybridization analysis (Figure 1b).

Detection of AML1-LAF4 *genomic junctions*

Southern blot analysis using a cDNA probe within exon 7 of *AML1* detected a rearranged band derived from an

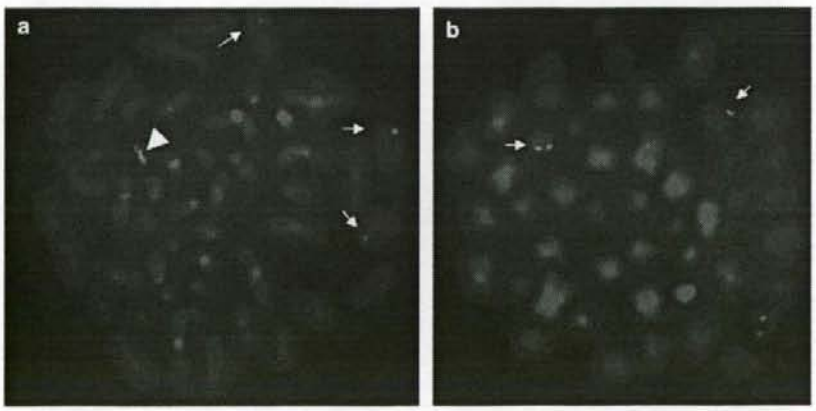

Figure 1 Fluorescence *in situ* hybridization analysis of the leukemic metaphase. **(a)** Both RP11-272A3 (green, 3′ side of *AML1*) and RP11-994N6 (red, 5′ side of *AML1*) were hybridized to normal chromosome 21 (arrowhead), RP11-272A3 to der(21)t(2;21)(q11.2;q22) (arrow, green signal) and RP11-994N6 to two der(2)t(2;21)(q11.2;q22) chromosomes (arrows, red signal). **(b)** Two fusion signals of RP11-994N6 (5′ of *AML1*, red signals) and RP11-527J8 (3′ of *LAF4*, green signals) were detected on two der(2)t(2;21)(q11.2;q22) chromosomes (arrows).

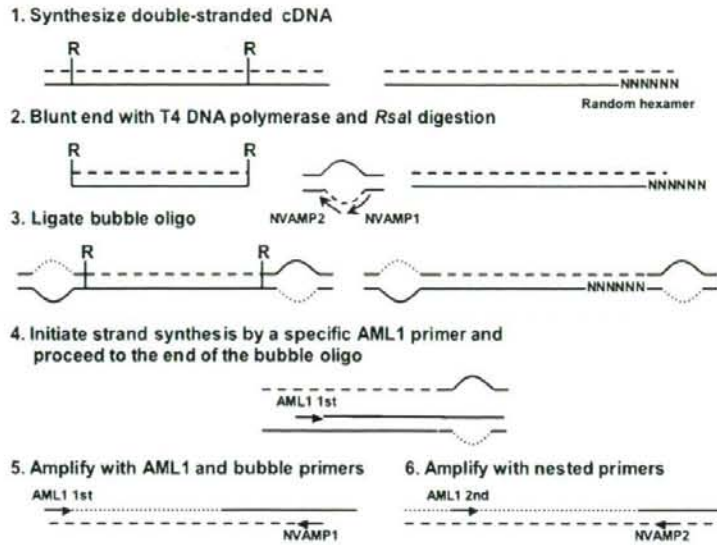

Figure 2 Outline of bubble PCR for cDNA. Bubble PCR primers (NVAMP-1 and NVAMP-2) can only anneal with one complementary sequence for bubble oligo synthesized with *AML1* primer, but not bubble oligo itself; therefore, this single-stranded bubble provides the specificity of the reaction.

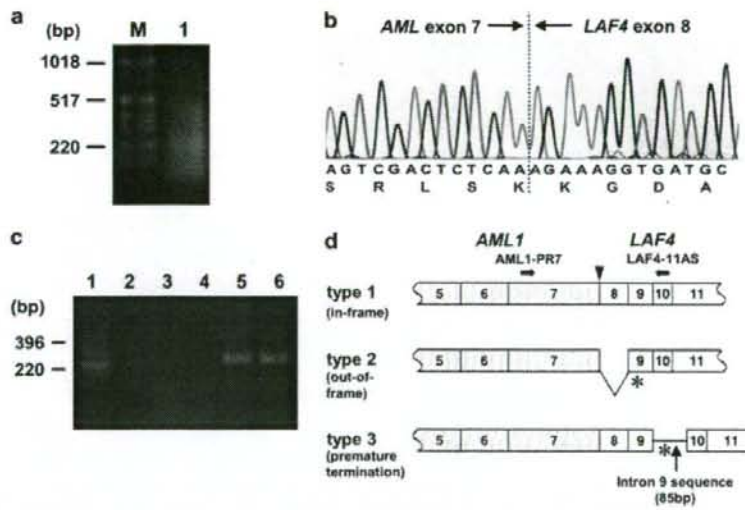

Figure 3 Identification of *AML1-LAF4* fusion transcript. (**a**) Bubble PCR products by nested PCR using AML1-5S and NVAMP1 for first PCR, and AML1-E6S and NVAMP2 for second PCR (lane 1). M, size marker. (**b**) Sequence analysis of *AML1-LAF4* fusion transcript. The single letter amino-acid sequences surrounding the fusion point are shown at the bottom of the figure. (**c**) Detection of *AML1-LAF4* fusion transcripts by reverse transcription-PCR. Primers were AML1-PR7 and LAF4-11AS (lanes 1 and 3), AML1-PR8 and LAF4-PR5 (lanes 2 and 4), and β-actin, respectively. Lanes 1, 3 and 5, patient's leukemic cells; lanes 2, 4 and 6, normal peripheral lymphocytes. (**d**) Three fusion transcripts of *AML1-LAF4* are schematically depicted. Gray/dotted boxes denote predicted *AML1* exons and white boxes represent predicted *LAF4* exons. Type 3 contains the *LAF4* intron 9 splicing donor site. AML1-PR7 and LAF4-11AS indicate the primers used for reverse transcription-PCR. Asterisk shows the termination codon.

approximately 11 kb *Bgl*II germline fragment on chromosome 21 (data not shown). To isolate the fusion point of chromosomes 2 and 21, we next performed bubble PCR on genomic DNA and detected nested PCR products using primers AML1-GNM8-2S and NVAMP2 (Figure 4a). Sequence analysis of the subcloned PCR product revealed the genomic junction of 5′-*AML1-LAF4*-3′ (Figures 4c and d), and the result

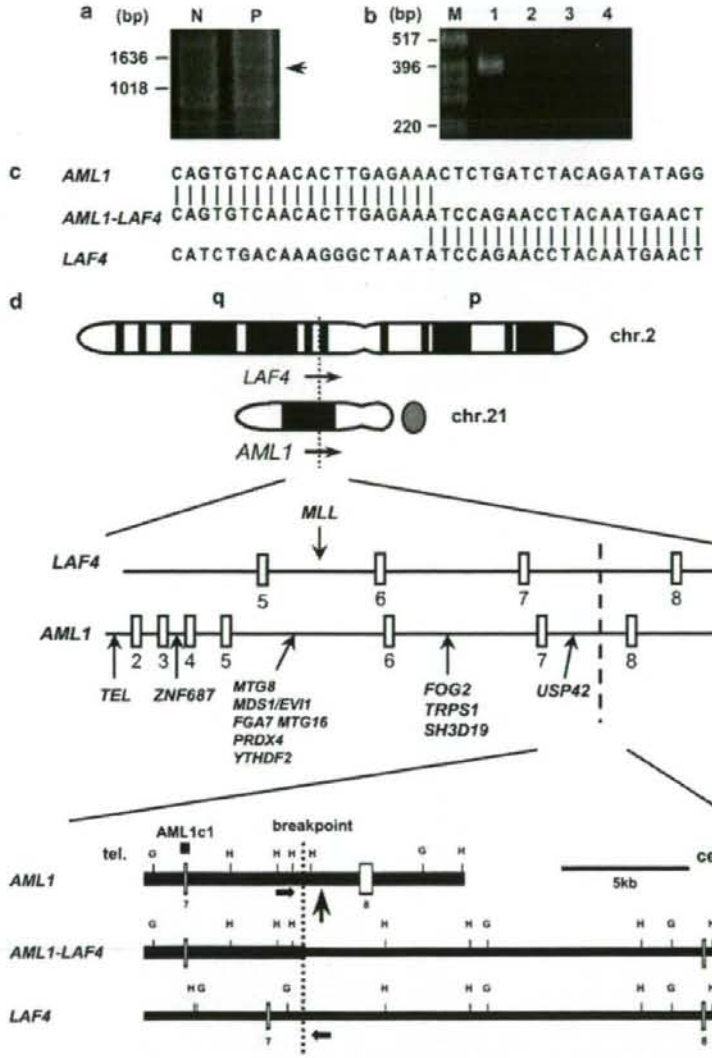

Figure 4 Cloning of the genomic junction of *AML1* and *LAF4*. (**a**) Bubble PCR for genomic DNA. N, normal human lymphocytes; P, patient's leukemic cells. (**b**) Detection of the genomic fusion point of *AML1-LAF4* by PCR. Primers were AML1-GNM8-4S and LAF4-GNM11-2AS (lanes 1 and 3), and LAF4-GNM11-2S and AML1-GNM8-2AS (lanes 2 and 4). Lanes 1 and 2, patient's leukemic cells; lanes 3 and 4, normal peripheral lymphocytes. M, size marker. (**c**) Sequences of breakpoints in the patient's leukemic cells. (**d**) Physical map of the breakpoint regions. Open vertical boxes represent defined exons in each gene. Horizontal arrows show the primers used. Restriction sites are indicated by capital letters: G, *Bgl*II; H, *Hin*dIII. AML1c1 indicates the position of the cDNA probes for Southern blot analysis. A vertical arrow shows *AML1-USP42* breakpoint.

was confirmed by PCR analysis using primers AML1-GNM8-4S and LAF4-GNM11-2AS (Figure 4b); however, no 5′-*LAF4-AML1*-3′ product was generated, suggesting interstitial deletion near genomic break points (Figure 4b). These sequences near the break points did not contain any lymphoid heptamer/nonamer sequences, *Alu* sequences or consensus topoisomerase II cleavage sites.

Discussion

In this study, we identified that *LAF4* was fused to *AML1* in pediatric T-ALL with t(2;21)(q11;q22). Other regions with chromosomal aberrations in this patient were not considered to be associated with recurrent cytogenetic changes involving T-ALL, except for the deletion of the short arm of chromosome 9. Spectral

karyotyping analysis detected del(9)(p13), and additional analysis of genome array (Human Mapping 50 K Hind Array, Affymetrix, Tokyo, Japan) revealed homozygous deletion of 4.5 Mb within the 9p21 region, including the *CDKN2A/p16/p14* locus (data not shown), which is frequently deleted in T-ALL (Ohnishi *et al.*, 1995).

Although the patient showed a complex chromosomal abnormality, t(2;21)(q11;q22) can form regular head-to-tail fusion transcripts of both *AML1* and *LAF4*, because the transcription direction of *AML1* and *LAF4* is telomere to centromere. Furthermore, fluorescence *in situ* hybridization analysis revealed two der(2)t(2;21)(q11.2;q22) creating 5′-*AML1-LAF4*-3′, suggesting that 5′-*AML1-LAF4*-3′ is critical for leukemogenesis.

LAF4 was previously reported to be a fusion partner of *MLL* in pediatric B-precursor ALL with t(2;21)(q11;q23) (von Bergh *et al.*, 2002; Bruch *et al.*, 2003; Hiwatari *et al.*, 2003). *LAF4* is the first gene fused to both *AML1* and *MLL*, and both *AML1-LAF4* and *MLL-LAF4* contained the same domains of *LAF4* (Figure 5). During the preparation of this manuscript, we found another pediatric T-ALL patient with *AML1-LAF4* reported in the Meeting Abstract (Abe *et al.*, *Blood* (ASH Annual Meeting Abstracts) 2006; **108**: 4276), suggesting that t(2;21)(q11;q23) is a recurrent cytogenetic abnormality and that the *AML1-LAF4* fusion gene is associated with the T-ALL phenotype. Both putative fusion proteins of AML1-LAF4 observed in two patients contained the Runt domain of AML1, and the transactivation domain, nuclear localization sequence and C-terminal homology domain of LAF4, although the fused exon of *LAF4* differed in the two cases. Several studies have reported that the fusion partners of *MLL* fused with different genes such as *MLL-AF10* and *CALM-AF10*, *MLL-CBP* and *MOZ-CBP* or *MLL-p300* and *MOZ-p300* (Ida *et al.*, 1997; Taki *et al.*, 1997; Chaffanet *et al.*, 2000). Comparison of the structure and function between *AML1-LAF4* and *MLL-LAF4* will facilitate our understanding of the molecular mechanisms underlying *AML1*- and *MLL*-related leukemia.

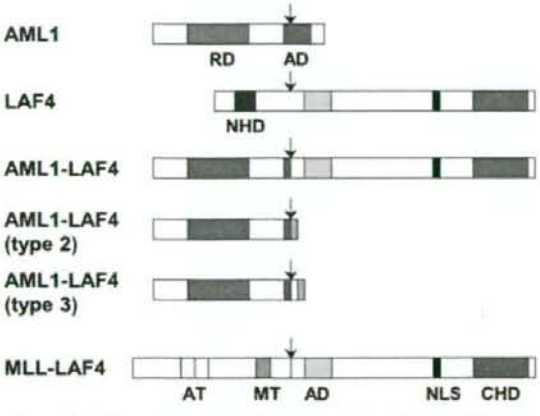

Figure 5 Schematic representation of putative AML1, LAF4 and AML1-LAF4 fusion proteins. Putative MLL-LAF4 fusion protein is also indicated for comparison. Arrows, break points or fusion points; AD, transactivation domain; AT, AT hooks; CHD, C-terminal homology domain; DNA, methyltransferase homology region; RD, RUNT domain; MT, DNA methyltransferase homology region; NLS, nuclear localization sequence.

The only *AML1* fusion partners in T-ALL are *LAF4* and *FGA7*. It is not known how *FGA7* is associated with T-ALL leukemogenesis, because *FGA7* does not show any significant sequence homology to any known protein motifs and/or domains (Mikhail *et al.*, 2004). Both patients with *AML1-LAF4* and *MLL-LAF4* fusions were diagnosed as having ALL, but they have different lymphoid lineages. *MLL-LAF4* is associated with B-lineage ALL; however, *AML1-LAF4* generates T-ALL. Our previous study showed that *LAF4* was expressed not only in B-lineage ALL but also in T-lineage ALL cell lines (Hiwatari *et al.*, 2003). *LAF4* showed strong sequence similarity to *AF4* (Ma and Staudt, 1996), which has a role in the differentiation of both B and T cells in mice (Isnard *et al.*, 2000). Furthermore, it was reported that *AML1* also plays an important role in T- and B-cell differentiation, because *AML1*-deficient bone marrow increased defective T- and B-lymphocyte development (Ichikawa *et al.*, 2004). These findings support that both *AML1* and *LAF4* are associated with T-ALL, respectively. Further functional analysis of the *AML1-LAF4* fusion gene will provide new insights into the leukemogenesis of *AML1*-related T-ALL. Recently, it has been reported that C-terminal truncated AML1-related fusion proteins play critical roles in leukemogenesis (Yan *et al.*, 2004, Agerstam *et al.*, 2007), suggesting that the two additional types of fusion transcripts observed in our patient (types 2 and 3 in Figures 3d and 5) have an additional function in leukemogenesis other than that of the entire AML1-LAF4 fusion protein.

In this study, we first applied the panhandle PCR method, which is usually used for cloning the fusion partners of *MLL* or *NUP98* (Megonigal *et al.*, 2000; Taketani *et al.*, 2002); however, no fusion transcripts could be obtained. Therefore, we searched for another method to clone the fusion transcripts and adapted the bubble PCR method for cDNA cloning. To date, bubble PCR has been performed for cloning unknown genomic fusion points but not fusion cDNAs (Zhang *et al.*, 1995). Using double-stranded cDNA, we could apply the bubble PCR method for cloning fusion cDNA with fewer nonspecific products. The bubble PCR primer can only prime DNA synthesis after a first-strand cDNA has been generated by an *AML1*-specific primer because of the bubble-tag with an internal non-complementary region (Zhang *et al.*, 1995). Although bubble PCR for genomic DNA generated one or two amplification products (Smith, 1992), bubble PCR for cDNA generated a complex set of amplification products that appeared as a smear by SYBR green staining, suggesting that a random hexamer generated various double-stranded cDNA containing the *AML1* sequence. This means that various fusion points can be estimated, even if after bubble oligo ligation was generated. Furthermore, bubble PCR for cDNA could amplify in both 5′–3′ and 3′–5′ directions of the gene or transcript, and easily

Table 1 Comparison between bubble PCR and panhandle PCR

Characteristics	*Bubble PCR*	*Panhandle PCR*
Available orientation of fusion transcript	5′–3′, 3′–5′	Only 5′–3′
AML1-specific random hexamer[a]	Not necessary	Necessary
Self-annealing	Not necessary	Necessary
Number of required polymerase reaction	2	4
Number of final products	Many (smear)	A few
Nonspecific product	Few	Few
Number of extra sequences other than targeted sequences in cloned product	50–60 bp	>100 bp
Search for other targeted exons	Easy	Hard[b]

[a]30-mers *AML1*-specific oligonucleotide with random hexamer (AML1-N). [b]Necessary to use another *AML1*-specific random hexamer if the target exons are 5′ region of the initial target.

handle any exons fused to unknown partners for amplification. Once-ligated cDNAs are also available for cloning any genes, other than *AML1*, as the target. We demonstrated the efficiency and specificity of bubble PCR for cDNA (Table 1 and Supplementary Figure S2).

To date, a great number of fusion genes associated with chromosomal translocations have been cloned, although these fusion genes are found as a minor part of various malignancies. Recently, high frequencies of mutations in *NOTCH1* in T-ALL (James *et al*., 2005), *NPM* in AML with normal karyotype (Weng *et al*., 2004) and *JAK2* in myeloproliferative disorders (polycythemia vera, essential thrombocythemia and idiopathic myelofibrosis) (James *et al*., 2005) have been reported, and these mutations are considered to be a good target for therapy. These genes were first identified as associated with chromosomal translocations in a small subset of specific phenotypes of hematologic malignancies (Ellisen *et al*., 1991; Morris *et al*., 1994; Lacronique *et al*., 1997). These findings suggest that continuing attempts to identify genes associated with chromosomal translocations can be expected to provide further insights into the significance of various gene alterations in cancer and the development of novel-targeted therapies (Taki and Taniwaki, 2006). The bubble PCR method for cDNA will contribute to identifying numerous novel translocation partners more easily and further functional analysis of chimeric transcripts.

Materials and methods

Spectral karyotyping analysis
Spectral karyotyping analysis was performed with a Sky-Painting kit (Applied Spectral Imaging, Migdal Ha'Emek, Israel). Signal detection was performed according to the manufacturer's instructions.

Fluorescence in situ *hybridization analysis*
Fluorescence *in situ* hybridization analysis of the patient's leukemic cells using *AML1*-specific BAC clones (RP11-272A3, 3′ of *AML1* and RP11-994N6, 5′ of *AML1*) was carried out as described previously (Taniwaki *et al*., 1994). Fusion of *AML1* and *LAF4* was analysed with the patient's leukemic cells using RP11-994N6 (5′ of *AML1*) and RP11-527J8 (3′ of *LAF4*).

Bubble PCR for cDNA
We modified the original bubble PCR method to apply for cDNA cloning (Figure 2; Supplementary Figure S2) (Smith, 1992; Zhang *et al*., 1995).

Poly(A)$^+$ RNA was extracted from the patient's leukemic cells using a QuickPrep Micro mRNA Purification Kit (GE Healthcare, Buckinghamshire, UK). Two hundred nanograms of poly(A)$^+$ RNA was reverse transcribed to cDNA in a total volume of 33 μl with random hexanucleotide using the Ready-To-Go You-Prime First-Strand Beads (GE Healthcare). Double-stranded cDNAs were synthesized from 10 μl of single-stranded cDNA with a phosphorylated random hexanucleotide, blunt ended with T4 DNA polymerase, digested with *Rsa*I endonuclease and ligated with bubble oligo. *Rsa*I, a 4-bp blunt-ended cutter, was chosen to shorten the bubble oligo-ligated fragments, so that almost all bubble oligo-ligated fragments would be easy to clone by standard PCR reaction. This suggests that poor-quality samples are also suited to this method, although it is unsuitable for cloning long products.

The sequences of the primers used are listed in Supplementary Table S1 and their positions in the *AML1* gene are shown in Supplementary Figure S2. Nested PCR was performed using primers NVAMP-1 (bubble oligo) and AML1-5S (exon 5) for first round PCR, and NVAMP-2 (bubble oligo) and AML1-E6S (exon 6) for nested PCR. NVAMP1 and NVAMP2 can only anneal to the newly synthesized unique sequence of the bubble oligo by AML1-5S.

We used poly(A)$^+$ RNA in bubble PCR for cDNA with the expectation that this approach could amplify fewer transcripts; however, total RNA is also suitable for this method.

Bubble PCR for genomic DNA
Bubble PCR for genomic DNA was performed as described previously (Smith, 1992; Zhang *et al*., 1995). Primers were as follows: NVAMP-1 and AML1-GNM8S for first round PCR, and NVAMP-2 and AML1-GNM8-2S for second round PCR (Supplementary Table S1).

Reverse transcription–PCR and genomic PCR analyses
Reverse transcription–PCR and genomic PCR analyses were performed as described previously. After 35 rounds of PCR (30 s at 94 °C, 30 s at 55 °C, 1 min at 72 °C), 5μl of PCR product were electrophoresed in a 3% agarose gel. Primers were as follows: AML1-PR7 and LAF4-11AS, and AML1-PR8 and LAF4-PR5 for reverse transcription-PCR; and AML1-GNM8-4S and LAF4-GNM11-2AS, and LAF4-GNM11-2S and AML1-GNM8-2AS for genomic PCR (Supplementary Table S1).

Nucleotide sequencing
Nucleotide sequences of PCR products and, if necessary, subcloned PCR products were analysed as described previously (Hiwatari *et al*., 2003).

Southern blot analysis
High-molecular-weight DNA was extracted from the patient's leukemic cells by proteinase K digestion and phenol/chloroform extraction. DNA (10 μg) was digested with *Bgl*II, subjected to electrophoresis on 0.7% agarose gel and transferred to a nylon membrane. Blots were hybridized to probes that were labeled by the Dig-labeled PCR method according to the manufacturer's instructions (Roche Applied Science, Tokyo, Japan). Probes

were 112 bp *AML1* cDNA fragments (AML1c1, nucleotides 1233–1344; GenBank accession no. NM_001754).

Abbreviations

AML, acute myeloid leukemia; ALL, acute lymphoblastic leukemia.

Acknowledgements

We express our appreciation for the outstanding technical assistance of Kozue Sugimoto, Minako Goto and Kayoko Kurita. This work was supported by a grant-in-aid for Scientific Research (B) from the Ministry of Education, Culture, Sports, Science and Technology of Japan, and the Takeda Science Foundation.

References

Agerstam H, Lilljebjorn H, Lassen C, Swedin A, Richter J, Vandenberghe P *et al.* (2007). Fusion gene-mediated truncation of *RUNX1* as a potential mechanism underlying disease progression in the 8p11 myeloproliferative syndrome. *Genes Chromosomes Cancer* **46**: 635–643.

Asou N, Yanagida M, Huang L, Yamamoto M, Shigesada K, Mitsuya H *et al.* (2007). Concurrent transcriptional deregulation of AML1/RUNX1 and GATA factors by the *AML1-TRPS1* chimeric gene in t(8;21)(q24;q22) acute myeloid leukemia. *Blood* **109**: 4023–4027.

Bruch J, Wilda M, Teigler-Schlegel A, Harbott J, Borkhardt A, Metzler M. (2003). Occurrence of an *MLL/LAF4* fusion gene caused by the insertion ins(11;2)(q23;q11.2q11.2) in an infant with acute lymphoblastic leukemia. *Genes Chromosomes Cancer* **37**: 106–109.

Chaffanet M, Gressin L, Preudhomme C, Soenen-Cornu V, Birnbaum D, Pebusque MJ. (2000). *MOZ* is fused to *p300* in an acute monocytic leukemia with t(8;22). *Genes Chromosomes Cancer* **28**: 138–144.

Chan EM, Comer EM, Brown FC, Richkind KE, Holmes ML, Chong BH *et al.* (2005). *AML1-FOG2* fusion protein in myelodysplasia. *Blood* **105**: 4523–4526.

Ellisen LW, Bird J, West DC, Soreng AL, Reynolds TC, Smith SD *et al.* (1991). *TAN-1*, the human homolog of the Drosophila *Notch* gene, is broken by chromosomal translocations in T lymphoblastic neoplasms. *Cell* **66**: 649–661.

Erickson P, Gao J, Chang KS, Look T, Whisenant E, Raimondi S *et al.* (1992). Identification of breakpoints in t(8;21) acute myelogenous leukemia and isolation of a fusion transcript, AML1/ETO, with similarity to *Drosophila* segmentation gene, runt. *Blood* **80**: 1825–1831.

Gamou T, Kitamura E, Hosoda F, Shimizu K, Shinohara K, Hayashi Y *et al.* (1998). The partner gene of *AML1* in t(16;21) myeloid malignancies is a novel member of the *MTG8* (*ETO*) family. *Blood* **91**: 4028–4037.

Golub TR, Barker GF, Bohlander SK, Hiebert SW, Ward DC, Bray-Ward P *et al.* (1995). Fusion of the *TEL* gene on 12p13 to the *AML1* gene on 21q22 in acute lymphoblastic leukemia. *Proc Natl Acad Sci USA* **92**: 4917–4921.

Grimwade D, Walker H, Oliver F, Wheatley K, Harrison C, Harrison G *et al.* (1998). The importance of diagnostic cytogenetics on outcome in AML: analysis of 1,612 patients entered into the MRC AML 10 trial. The Medical Research Council Adult and Children's Leukaemia Working Parties. *Blood* **92**: 2322–2333.

Hayashi Y. (2000). The molecular genetics of recurring chromosome abnormalities in acute myeloid leukemia. *Semin Hematol* **37**: 368–380.

Hiwatari M, Taki T, Taketani T, Taniwaki M, Sugita K, Okuya M *et al.* (2003). Fusion of an *AF4*-related gene, *LAF4*, to *MLL* in childhood acute lymphoblastic leukemia with t(2;11)(q11;q23). *Oncogene* **22**: 2851–2855.

Ichikawa M, Asai T, Saito T, Seo S, Yamazaki I, Yamagata T *et al.* (2004). *AML-1* is required for megakaryocytic maturation and lymphocytic differentiation, but not for maintenance of hematopoietic stem cells in adult hematopoiesis. *Nat Med* **10**: 299–304.

Ida K, Kitabayashi I, Taki T, Taniwaki M, Noro K, Yamamoto M *et al.* (1997). Adenoviral E1A-associated protein p300 is involved in acute myeloid leukemia with t(11;22)(q23;q13). *Blood* **90**: 4699–4704.

Isnard P, Core N, Naquet P, Djabali M. (2000). Altered lymphoid development in mice deficient for the m*AF4* proto-oncogene. *Blood* **96**: 705–710.

James C, Ugo V, Le Couedic JP, Staerk J, Delhommeau F, Lacout C *et al.* (2005). A unique clonal *JAK2* mutation leading to constitutive signalling causes polycythaemia vera. *Nature* **434**: 1144–1148.

Kurokawa M, Hirai H. (2003). Role of AML1/Runx1 in the pathogenesis of hematological malignancies. *Cancer Sci* **94**: 841–846.

Lacronique V, Boureux A, Valle VD, Poirel H, Quang CT, Mauchauffe M *et al.* (1997). A TEL-JAK2 fusion protein with constitutive kinase activity in human leukemia. *Science* **278**: 1309–1312.

Ma C, Staudt LM. (1996). *LAF-4* encodes a lymphoid nuclear protein with transactivation potential that is homologous to *AF-4*, the gene fused to *MLL* in t(4;11) leukemias. *Blood* **87**: 734–745.

Megonigal MD, Rappaport EF, Wilson RB, Jones DH, Whitlock JA, Ortega JA *et al.* (2000). Panhandle PCR for cDNA: a rapid method for isolation of *MLL* fusion transcripts involving unknown partner genes. *Proc Natl Acad Sci USA* **97**: 9597–9602.

Mikhail FM, Coignet L, Hatem N, Mourad ZI, Farawela HM, El Kaffash DM *et al.* (2004). *FGA7*, is fused to *RUNX1/AML1* in a t(4;21)(q28;q22) in a patient with T-cell acute lymphoblastic leukemia. *Genes Chromosomes Cancer* **39**: 110–118.

Mitani K, Ogawa S, Tanaka T, Miyoshi H, Kurokawa M, Mano H *et al.* (1994). Generation of the *AML1-EVI-1* fusion gene in the t(3;21)(q26;q22) causes blastic crisis in chronic myelocytic leukemia. *EMBO J* **13**: 504–510.

Miyoshi H, Kozu T, Shimizu K, Enomoto K, Maseki N, Kaneko Y *et al.* (1993). The t(8;21) translocation in acute myeloid leukemia results in production of an *AML1-MTG8* fusion transcript. *EMBO J* **12**: 2715–2721.

Miyoshi H, Shimizu K, Kozu T, Maseki N, Kaneko Y, Ohki M. (1991). t(8;21) breakpoints on chromosome 21 in acute myeloid leukemia are clustered within a limited region of a single gene, *AML1*. *Proc Natl Acad Sci USA* **88**: 10431–10434.

Morris SW, Kirstein MN, Valentine MB, Dittmer KG, Shapiro DN, Saltman DL *et al.* (1994). Fusion of a kinase gene, *ALK*, to a nucleolar protein gene, *NPM*, in non-Hodgkin's lymphoma. *Science* **263**: 1281–1284.

Nguyen TT, Ma LN, Slovak ML, Bangs CD, Cherry AM, Arber DA. (2006). Identification of novel *Runx1* (*AML1*) translocation partner genes *SH3D19*, *YTHDf2*, and *ZNF687* in acute myeloid leukemia. *Genes Chromosomes Cancer* **45**: 918–932.

Ohnishi H, Kawamura M, Ida K, Sheng XM, Hanada R, Nobori T *et al.* (1995). Homozygous deletions of *p16/MTS1* gene are frequent but mutations are infrequent in childhood T-cell acute lymphoblastic leukemia. *Blood* **86**: 1269–1275.

Okuda T, Cai Z, Yang S, Lenny N, Lyu CJ, van Deursen JM *et al.* (1998). Expression of a knocked-in *AML1-ETO* leukemia gene inhibits the establishment of normal definitive hematopoiesis and directly generates dysplastic hematopoietic progenitors. *Blood* **91**: 3134–3143.

Paulsson K, Bekassy AN, Olofsson T, Mitelman F, Johansson B, Panagopoulos I. (2006). A novel and cytogenetically cryptic t(7;21)(p22;q22) in acute myeloid leukemia results in fusion of *RUNX1* with the ubiquitin-specific protease gene *USP42*. *Leukemia* **20**: 224–229.

Rowley JD. (1999). The role of chromosome translocations in leukemogenesis. *Semin Hematol* **36**: 59–72.

Smith DR. (1992). Ligation-mediated PCR of restriction fragments from large DNA molecules. *PCR Methods Appl* **2**: 21–27.

Taketani T, Taki T, Shibuya N, Ito E, Kitazawa J, Terui K *et al.* (2002). The *HOXD11* gene is fused to the *NUP98* gene in acute myeloid leukemia with t(2;11)(q31;p15). *Cancer Res* **62**: 33–37.

Taki T, Sako M, Tsuchida M, Hayashi Y. (1997). The t(11;16)(q23;p13) translocation in myelodysplastic syndrome fuses the *MLL* gene to the *CBP* gene. *Blood* **89**: 3945–3950.

Taki T, Taniwaki M. (2006). Chromosomal translocations in cancer and their relevance for therapy. *Curr Opin Oncol* **18**: 62–68.

Taniwaki M, Matsuda F, Jauch A, Nishida K, Takashima T, Tagawa S *et al.* (1994). Detection of 14q32 translocations in B-cell malignancies by *in situ* hybridization with yeast artificial chromosome clones containing the human IgH gene locus. *Blood* **83**: 2962–2969.

Von Bergh AR, Beverloo HB, Rombout P, van Wering ER, van Weel MH, Beverstock GC *et al.* (2002). *LAF4*, an *AF4*-related gene, is fused to *MLL* in infant acute lymphoblastic leukemia. *Genes Chromosomes Cancer* **37**: 106–109.

Wang J, Hoshino T, Redner RL, Kajigaya S, Liu JM. (1998). *ETO*, fusion partner in t(8;21) acute myeloid leukemia, represses transcription by interaction with the human N-CoR/mSin3/HDAC1 complex. *Proc Natl Acad Sci USA* **95**: 10860–10865.

Weng AP, Ferrando AA, Lee W, Lee W, Morris IV JP, Silverman LB *et al.* (2004). Activating mutations of *NOTCH1* in human T cell acute lymphoblastic leukemia. *Science* **306**: 269–271.

Yan M, Burel SA, Peterson LF, Kanbe E, Iwasaki H, Boyapati A *et al.* (2004). Deletion of an AML1-ETO C-terminal NcoR/SMRT-interacting region strongly induces leukemia development. *Proc Natl Acad Sci USA* **101**: 17186–17191.

Zhang JG, Goldman JM, Cross NC. (1995). Characterization of genomic *BCR-ABL* breakpoints in chronic myeloid leukemia by PCR. *Br J Haematol* **90**: 138–146.

Zhang Y, Emmanuel N, Kamboj G, Chen J, Shurafa M, Van Dyke DL *et al.* (2004). *PRDX4*, a member of the peroxiredoxin family, is fused to *AML1* (*RUNX1*) in an acute myeloid leukemia patient with a t(X;21)(p22;q22). *Genes Chromosomes Cancer* **40**: 365–370.

Supplementary Information accompanies the paper on the Oncogene website (http://www.nature.com/onc).

Available online at www.sciencedirect.com
ScienceDirect
Leukemia Research 32 (2008) 1462–1467
Leukemia Research
www.elsevier.com/locate/leukres

Brief communication

Fully automated and super-rapid system for the detection of JAK2V617F mutation

Ruriko Tanaka [a,1], Junya Kuroda [b,1], William Stevenson [c], Eishi Ashihara [a], Takayuki Ishikawa [d], Tomohiko Taki [e], Yutaka Kobayashi [f], Yuri Kamitsuji [a,b], Eri Kawata [a,b], Miki Takeuchi [a], Yoshihide Murotani [a], Asumi Yokota [a], Mitsuharu Hirai [g], Satoshi Majima [g], Masafumi Taniwaki [b], Taira Maekawa [a], Shinya Kimura [a,*]

[a] Department of Transfusion Medicine and Cell Therapy, Kyoto University Hospital, 54 Shogoin Kawahara-cho, Sakyo-ku, Kyoto 606-8507, Japan
[b] Division of Hematology and Oncology, Department of Medicine, Kyoto Prefectural University of Medicine, Kajii-cho, Kamigyo-ku, Kyoto 602-8566, Japan
[c] Department of Haematology, Royal North Shore Hospital, St Leonards, New South Wales 2065, Australia
[d] Department of Hematology and Oncology, Graduate School of Medicine, Kyoto University, hogoin Kawahara-cho, Sakyo-ku, Kyoto 606-8507, Japan
[e] Department of Molecular Laboratory Medicine, Kyoto Prefectural University of Medicine, Kajii-cho, Kamigyo-ku, Kyoto 602-8566, Japan
[f] Division of Hematology, Department of Medicine, Kyoto Second Red Cross Hospital, Haruobi-cho, Kamigyo-ku, Kyoto 602-8026, Japan
[g] ARKRAY, Inc., Takanna-cho, Nakagyo-ku, Kyoto 604-8153, Japan

Received 7 November 2007; received in revised form 28 December 2007; accepted 31 December 2007
Available online 6 March 2008

Abstract

JAK2V617F is a common mutation in chronic myeloproliferative diseases (CMPDs). We have developed a system utilizing JAK2V617F-specific guanine quenching probe (QP-system) to detect JAK2V617F. With QP-system, results can be obtained from 100 μl of blood within 90 min. We compared QP-system with direct sequencing using 42 CMPD patients' specimens. JAK2V617F was detected in 25 specimens by QP-system, while direct sequencing failed to detect JAK2V617F in 7 of those 25. The presence of JAK2V617F mutation in these 7 specimens was confirmed by allele-specific PCR. These findings indicate that QP-system is more sensitive and useful than direct sequencing for diagnoses of CMPDs.

Keywords: JAK2; V617F; Chronic myeloproliferative diseases; Guanine quenching probe; Direct sequencing

1. Introduction

A single G to T somatic point mutation at nucleotide 1849 in exon 14 of the *jak2* gene results in the substitution of valine to phenylalanine at codon 617. This mutation, designated JAK2V617F, has been identified in most polycythemia vera (PV) patients, approximately half of essential thrombocythemia (ET) and chronic idiopathic myelofibrosis with extramedullary hematopoiesis (CIMF) patients, and in a substantial population of other chronic myeloproliferative disease (CMPD) patients [1].

JAK2V617F is a gain-of-function mutation that stimulates JAK2 tyrosine kinase (TK) activity, leading to the abnormal clonal expansion of myeloid cells [2]. Before the JAK2V617F mutation was discovered, CMPDs had often been difficult to diagnose because of the considerable overlap of their clini-

* Corresponding author. Tel.: +81 75 751 3630; fax: +81 75 751 3631.
E-mail address: shkimu@kuhp.kyoto-u.ac.jp (S. Kimura).
[1] These authors have contributed equally to this work.

0145-2126/$ – see front matter © 2008 Elsevier Ltd. All rights reserved.
doi:10.1016/j.leukres.2007.12.019

Table 1
JAK2V617F analysis of patient specimens

No.	Age, sex	Dx.	Sample	Blood cell count			Treatment	Complication	JAK2V617F			
				WBC ($\times 10^9 l^{-1}$)	Hb (g/dl)	Plt ($\times 10^9 l^{-1}$)			QP	DS	AS	Mutant cell ratio (%)[a]
Patients with definite CMPDs												
1	73, M	uCMPD → PV	PB	16.4	17.7	759	HU	–	+	+		>20
2	79, M	PV	PB	21.8	18.3	817	HU	–	+	–	+	1–20
3	62, F	uCMPD → PV	DNA	12.9	15.4	414	–	–	+	+		1–20
4	59, F	PV	DNA	36.4	16.9	353	–	–	+	+		1–20
5	66, M	PV	PB	5.9	19.5	215	Phlebotomy	–	+	+		1–20
6	49, F	PV	PB	16.4	17.4	597	Phlebotomy	–	+	+		1–20
7	71, F	PV	PB	26.9	16.8	814	–	–	+	+		>20
8	77, M	PV	PB	19.0	19.6	570	HU, phlebotomy	–	+	+		>20
9	59, F	ET	DNA	10.0	15.0	1070	–	–	+	+		1–20
10	76, F	ET	PB	16.0	15.2	1140	BU	–	+	–	+	1–20
11	51, M	ET	DNA	17.5	12.2	822	–	–	–	–		0 or <1
12	73, F	ET	PB	32.0	12.8	2330	BU	–	+	+		1–20
13	33, F	ET	PB	6.0	13.3	1660	HU	–	–	–		0 or <1
14	80, F	ET	PB	33.3	8.0	900	–	–	+	+		>20
15	68, M	ET	PB	10.8	12.1	728	–	–	+	+		1–20
16	57, M	ET	PB	11.4	11.5	1210	–	Cerebral infarction	+	+		1–20
17	60, M	ET	PB	11.9	15.7	881	HU	–	+	+		>20
18	76, F	ET	PB	16.9	16.6	1210	HU	Ischemic colitis	+	+		1–20
19	64, M	ET	PB	17.0	12.0	900	–	Cerebral hemorrhage	–	–		0 or <1
20	60, F	ET	DNA	9.7	13.4	1310	–	–	–	–		0 or <1
21	34, F	ET	DNA	9.2	12.7	1160	–	–	–	–		0 or <1
22	73, M	ET	DNA	24.2	16.5	1870	SPAC	Arterial obstruction	+	–	+	1–20
23	77, F	ET	DNA	8.9	12.4	1570	–	–	+	–	+	1–20
24	57, M	ET	DNA	1.5	7.1	97	–	Secondary MF	–	–		0 or <1
25	65, F	ET	DNA	10.6	9.6	1120	HU	–	+	–	+	1–20
26	94, M	ET	DNA	8.8	10.6	1190	HU	–	–	–		0 or <1
27	81, M	ET	PB	NA	NA	1540	BU	–	–	–		0 or <1
28	82, M	ET	PB	6.7	15.6	1540	BU	–	–	–		0 or <1
29	68, F	ET	PB	9.3	9.9	889	–	–	–	–		0 or <1
30	37, F	ET	PB	10.0	10.8	1300	–	–	+	–	+	1–20
31	57, F	ET	PB	10.4	12.1	1540	–	–	+	–	+	1–20
32	55, F	ET	PB	6.1	15.2	548	–	–	+	+		1–20
33	69, M	CIMF	DNA	0.7	8.5	20	–	–	–	–		0 or <1
34	76, M	CMMoL	DNA	98.4	4.3	1550	HU, SPAC	–	+	+		1–20
35	81, F	CNL	PB	11.9	4.0	40	IFN-alpha	–	–	–		0 or <1
36	50, M	uCMPD	DNA	24.2	14.7	434	HU	–	+	+		1–20
37	74, M	uCMPD.	DNA	35.0	11.2	1450	HU	–	+	+		1–20
38	77, M	uCMPD	PB	65.4	11.5	160	Ara-C	–	–	–		0 or <1
39	72, M	uCMPD	DNA	20.0	13.6	428	–	–	–	–		0 or <1

Table 1 (*Continued*)

No.	Age, sex	Dx.	Sample	WBC ($\times 10^9 l^{-1}$)	Hb (g/dl)	Plt ($\times 10^9 l^{-1}$)	Treatment	Reason for BMT	QP	DS	AS	Mutant cell ratio (%)
Post-BMT patients												
40	61, F	CIMF	DNA	NA	NA	NA	BMT	Bone marrow failure	–	–		0 or <1
41	72, M	CIMF	DNA	3.2	7.9	97	BMT	Bone marrow failure	+	+		1–20
42	54, M	uCMPD	DNA	NA	NA	NA	BMT	Bone marrow failure	–	–		0 or <1

No.	Age, sex	Dx.	Sample	Abnormality in blood cell count	Treatment	Symptom, habbit	QP	DS	AS	Mutant cell ratio (%)
Secondary erythrocythemia										
43	75, M	SE	DNA	Hb 18.2 g/dl	–	–	–	–		0 or <1
44	61, M	SE	DNA	Hb 19.1 g/dl	–	Heavy smoking	–	–		0 or <1
45	58, M	SE	PB	Hb 17.5 g/l	–	Pickwick syndrome	–	–		0 or <1
Healthy volunteer										
46	45, M	healthy	PB	NA	–	–	–	–		
47	45, M	healthy	PB	NA	–	–	–	–		
48	36, M	healthy	PB	NA	–	–	–	–		

Abbreviation: Ara-C, cytarabine; QP, quenching probe system; AS, allele-specific PCR; BMT, allogeneic bone marrow transplantation; BU, busulfan; CIMF, chronic idiopathic myelofibrosis; CMMoL, chronic myelomonocytic leukemia; CMPDs, chronic myeloproliferative diseases; CNL, chronic neutrophilic leukemia; DS, direct sequencing; Dx., diagnosis; ET, essential thrombocythemia; HU, hydroxyurea; IFN, interferon; MF, myelofibrosis; PB, peripheral blood; PV, polycythemia vera; SPAC, cytarabine octosfate; SE, secondary erythrocythemia; uCMPD, unclassifiable chronic myeloproliferative disorder; NA, no data available.

* Measured by QP-system.

cal manifestations with secondary or reactive hypercytoses. However, the ability to detect this mutation now makes the diagnosis of CMPDs more straightforward [1]. The early identification of JAK2V617F is important because patients carrying this mutation have a higher incidence of leukemic transformation or thrombosis, and reduced survival, compared with CMPD patients that do not have this mutation [1]. JAK2V617F might also be a target for therapeutic intervention [2]. Thus, it is critical that this mutation can be accurately and rapidly detected. Here, we have developed a rapid, sensitive and fully automated JAK2V617F detection system utilizing a JAK2V617F-specific guanine quenching probe. We believe that this QP-system will be a valuable tool for the diagnoses of CMPDs.

2. Materials and methods

2.1. Cell lines and patient specimens

HEL is an acute leukemia cell line with the JAK2V617F mutation [2] and MYL is a chronic myelogenous leukemia-derived cell line with wild type JAK2 [3]. Patient samples were collected after receipt of informed consent, in accordance with the declaration of Helsinki. We tested 42 specimens from CMPD patients (no. 1–42) (Table 1) for JAK2V617F using both the QP-system and direct sequencing. The specimens were derived from 8 PV patients (including two patients those were initially diagnosed as unclassifiable CMPD (uCMPD) and re-diagnosed as PV later), 24 ET, 3 CIMF, 1 chronic myelomonocytic leukemia, 1 chronic neutrophilic leukemia and 5 uCMPD patients. Patients were diagnosed according to the latest WHO classification [4]. We also examined 3 samples from patients (no. 43–45) with secondary erythrocythemia that were suspected to have PV, and 3 healthy volunteers (no. 46–48).

2.2. Detection of JAK2V617F

The forward and reverse polymerase chain reaction (PCR) primers flanking *jak2* G1849 were 5′-gcagcaagtatgatgagcaagctttctc-3′ and 5′-gctctgagaaaggcattagaaagcctg-3′, respectively. The TAMRA-conjugated specific guanine quench fluorophore probe (QProbe, J-Bio21, Tokyo, Japan), which is complementary to mutant *jak2*, was 5′-agtatgtttctgtggagac-(TAMRA)-3′ (*jak2* 1842-1860). A prototype instrument for the QP-system was made by ARKRAY, Inc. (Kyoto, Japan) [5]. To detect the JAK2V617F in human specimens, a peripheral blood, bone marrow or DNA extract was added to a pre-treatment cartridge. A DNA binding matrix fragment with a form tipped applicator (FTA) tip (Whatman plc., Middlesex, UK) was dipped into the specimen using a robotic arm, and was then washed in three consecutive wells for a few minutes each while being shaken. The FTA tip containing the washed template was then transferred to the reagent cartridge where the template was first

denatured at 95 °C for 2 min and then mixed with primers, the QProbe and the PCR reaction mix reagents. The FTA tip was then transferred into a detection tube and Gene Taq FP (Nippon Gene, Co. Ltd., Toyama, Japan) was added before the tube was screw capped. The PCR was then initiated. A 5 s denaturation at 95 °C was followed by a 30 s annealing step at 58 °C, and this was repeated for 35–50 cycles, as required (Fig. 1 and Supplemental Fig. 1). In theory, the QProbe can bind to both wild type and mutant *jak2* amplicons during the PCR, but will preferentially bind to the mutated sequence with higher affinity. After the PCR was complete, the temperature was reduced to 40 °C and then was gradually increased. To identify wild type and mutated amplicons, the fluorescence intensity at different temperatures was measured; excitation at 485–555 nm and detection at 585–700 nm. An increase in fluorescence occurs when the QProbe dissociates from the amplicon. The QProbe dissociates from the wild type *jak2* amplicon at 52 °C but does not dissociate from mutant *jak2* until the temperature reaches 58 °C. Therefore, the mutant allele was present in samples in which a spike in fluorescence was observed at 58 °C (Fig. 2). All of these procedures were completed within 75 min (when 35 PCR cycles were used) or 90 min (50 PCR cycles). The val-

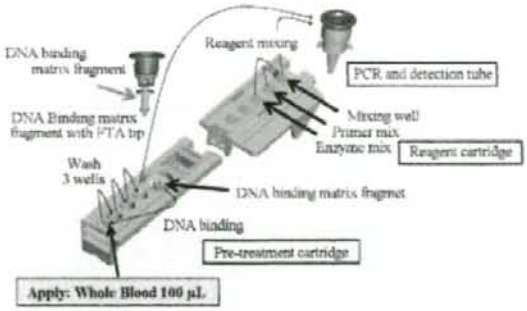

Fig. 1. The equipment utilized for QP-system. A FTA DNA binding matrix fragment is dipped into 100 µl of blood that has been applied to the pre-treatment cartridge. DNA from this blood specimen binds to the tip, which is then washed and subjected to a mixing step in the reagent cartridge. At this step the template DNA is mixed with PCR mix reagents, primers and the specific probe for mutant *jak2*. This sample is then added to the amplification/detection tube where the PCR is initiated automatically.

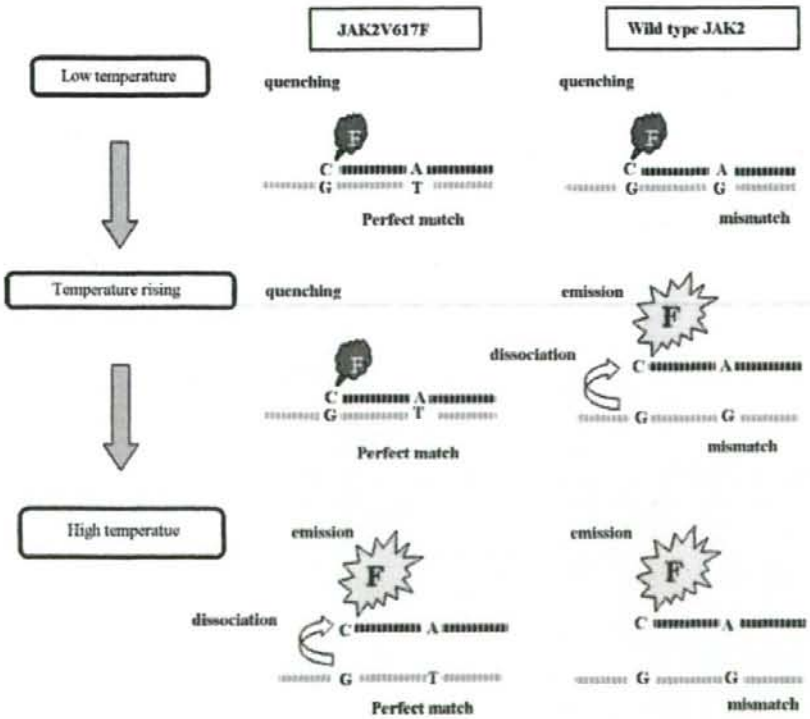

Fig. 2. Principle of QP-system. Detection of mutant and wild type *jak2* by the dissociation of the QProbe from the PCR amplicon. After completing the PCR, the temperature of each sample was reduced to 40 °C and then gradually increased. The QProbe dissociates from the wild type *jak2* amplicon at 52 °C and from the mutant *jak2* amplicon at 58 °C. The dissociation of the QProbe from the amplicons is measured by an increase in fluorescence.

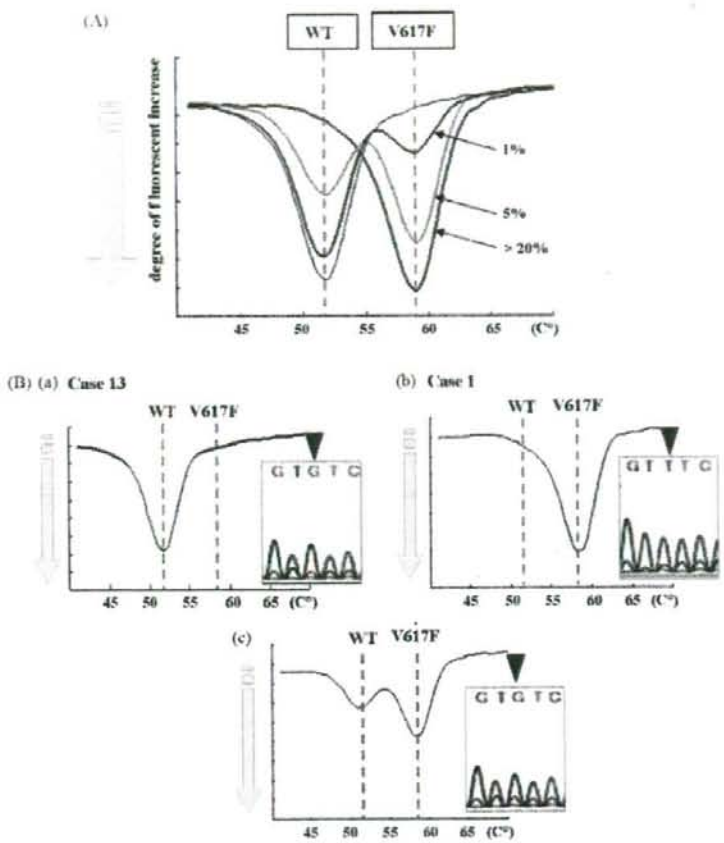

Fig. 3. (A) The sensitivity of JAK2V617F detection in QP-system. HEL cells containing mutant JAK2 and MYL cells containing wild type JAK2 were mixed in the following ratios (HEL:MYL): 0:100 (black), 1:99 (red), 5:95 (green) and 100:0 (blue). The traces are representative of five independent experiments. (B) Examples of JAK2V617F detection by QP-system and DNA direct sequencing in (a) an ET patient in which both methods confirm the absence of the JAK2V617F mutation (specimen #13 in Table 1), (b) a PV patient in which the JAK2V617F mutation was detected by both methods (specimen #1) and (c) an ET patient in which the mutation was detected by QP-system but not by direct sequencing (specimen #23).

ues of JAK2V617F measured by the QP-system were divided into three groups according to the results from the mixture of HEL and MYL cells (Fig. 3A). When one peak at the lower temperature (Fig. 3B(a)), two separate peaks (Fig. 3B(c)) and one peak at higher temperature (Fig. 3B(b)) were observed, the values of mutant cells were estimated as 0 or less than 1.0%, from 1.0% to 20% and more than 20%, respectively.

Direct sequencing and allele-specific PCR were performed as previously described [6].

3. Results and discussion

Several techniques have been utilized to detect the JAK2V617F mutation including denaturing high-performance liquid chromatography, direct sequencing, real-time PCR, TaqMan PCR single nucleotide polymorphism genotyping, pyrosequencing and allele-specific PCR. However, these approaches are often time-consuming and require a high level of individual technical skill and experience.

Wild type and mutant *jak2* can be easily distinguished by using the QP-system because the melting temperature of the mutant *jak2* amplicon is higher (58 °C) than the wild type *jak2* amplicons (52 °C) (Figs. 2 and 3). To verify the sensitivity of the QP-system, HEL and MYL cells were combined in different ratios. The QP-system detects small (1.0%) changes in the number of mutant cells present among wild type cells (Fig. 3), and its sensitivity is superior to or similar with other detection methods except allele-specific PCR. Because of its high sensitivity, allele-specific PCR sometimes produce false-positive results. Indeed, the cut-off level for the JAK2V617F detection was determined by the frequency of false-positive tests in allele-specific PCR [7]. The QP-